

Time-dependent simulations of steady C-type shocks

S. Van Loo,^{1*} I. Ashmore¹, P. Caselli¹, S. A. E. G. Falle², and T. W. Hartquist¹

¹ *School of Physics and Astronomy, University of Leeds, Leeds LS2 9JT, UK*

² *Department of Applied Mathematics, University of Leeds, Leeds LS2 9JT, UK*

Accepted - . Received - ; in original form -

ABSTRACT

Using a time-dependent multifluid, magnetohydrodynamic code, we calculated the structure of steady perpendicular and oblique C-type shocks in dusty plasmas. We included relevant processes to describe mass transfer between the different fluids, radiative cooling by emission lines and grain charging and studied the effect of single-sized and multiple sized grains on the shock structure. Our models are the first of oblique fast-mode molecular shocks in which such a rigorous treatment of the dust grain dynamics has been combined with a self-consistent calculation of the thermal and ionisation structures including appropriate microphysics. At low densities the grains do not play any significant rôle in the shock dynamics. At high densities, the ionisation fraction is sufficiently low that dust grains are important charge and current carriers and, thus, determine the shock structure. We find that the magnetic field in the shock front has a significant rotation out of the initial upstream plane. This is most pronounced for single-sized grains and small angles of the shock normal with the magnetic field. Our results are similar to previous studies of steady C-type shocks showing that our method is efficient, rigorous and robust. Unlike the method employed in the previous most detailed treatment of dust in steady oblique fast-mode shocks, ours allows a reliable calculation even when chemical or other conditions deviate from local statistical equilibrium. We are also able to model transient phenomena.

Key words: MHD – shock waves – ISM: dust – ISM: jets and outflows

1 INTRODUCTION

Molecular outflows associated with proto-stellar objects (e.g. Bally & Lada 1983) drive shocks into dark molecular clouds where the fractional ionisation χ is low ($\chi < 10^{-6}$). The low values of χ cause the gas and the magnetic field to be weakly coupled. Charged particles are then pushed through the neutral gas by Lorentz forces, giving rise to ambipolar diffusion (Mestel & Spitzer 1956). Collisions between the charged and neutral particles accelerate, compress and heat the neutral gas ahead of the shock front and a magnetic precursor forms. If the shock speed is low enough for the gas to cool efficiently, the flow becomes continuous in all fluids (e.g. Mullan 1971). Such shocks are referred to as C-type shocks (Draine 1980).

Draine, Roberge, & Dalgarno (1983, hereafter DRD) calculated the structures of steady perpendicular C-type shocks in diffuse and dense molecular media using a steady-state multifluid magnetohydrodynamic (MHD) description. They included a detailed treatment for energy and momentum transfer between different particles, oxygen-based chemistry and radiative cooling. They also assumed that the ion and electron densities exceed the grain charge density.

However, for a fractional ionisation below 10^{-7} , grains play an important rôle in governing the electromagnetic forces (Draine 1980). In the densest regions of molecular clouds where $n_H \geq 10^6 \text{ cm}^{-3}$, the fractional ionisation constraint is usually fulfilled.

Pilipp, Hartquist, & Havnes (1990) included the effect of dust grains on the structure of perpendicular steady C-type shocks more rigorously than previous authors (e.g. DRD). Their four-fluid models predict different shock widths than obtained in similar models of DRD. This model was extended to oblique shocks by Pilipp & Hartquist (1994) who found that in such shocks the transverse component of the magnetic field rotates about the propagation direction of the shock as long as there is a non-negligible Hall conductivity. This happens for a wide range of conditions, but Pilipp & Hartquist were unable to find solutions for fast-mode shocks.

Wardle (1998) pointed out that, to find a stable shock structure for steady oblique fast-mode shocks, one needs to integrate the steady state equations backwards in time from the downstream boundary. However, such a method requires an exact thermal, chemical and ionisation equilibrium. Such an equilibrium does not obtain in most shocks of interest. For instance, the abundance of water, an important coolant, is out of equilibrium for about 10^5 years or more from the

* E-mail: physvl@leeds.ac.uk

time the gas cools below several hundred degree. This highlights the necessity for time-dependent simulations to calculate the C-type shock structure. Ciolek & Roberge (2002) were the first to include a fluid description of grain dynamics in multifluid MHD simulations. However, their study is restricted to perpendicular shocks. The multifluid approach developed by Falle (2003) overcomes this limitation.

In this paper we study the structures of steady fast-mode C-type shocks using time-dependent multifluid MHD simulations. In Sect. 2 we describe the numerical code and the physical processes that we include. Then, we apply the code to perpendicular and oblique shocks with parameters similar to those of DRD including a single-sized grain fluid (Sect. 3) or multiple grain fluids (Sect. 4). Finally, we discuss the results and give our conclusions in Sect. 5.

2 THE MODEL

2.1 Numerical code

As the ionisation fraction within molecular clouds is low, the plasma needs to be treated as a multicomponent fluid consisting of neutrals, ions, electrons and N dust grain species. The governing equations for the neutral fluid are given by

$$\frac{\partial \rho_n}{\partial t} + \frac{\partial}{\partial x}(\rho_n v_{x,n}) = \sum_j s_{jn}, \quad (1)$$

$$\frac{\partial \rho_n \mathbf{v}_n}{\partial t} + \frac{\partial}{\partial x}(\rho_n v_{x,n} \mathbf{v}_n + p_n \mathbf{1}_x) = \frac{\mathbf{J} \times \mathbf{B}}{c}, \quad (2)$$

$$\frac{\partial e_n}{\partial t} + \frac{\partial}{\partial x} \left[v_{x,n} \left(e_n + p_n + \frac{1}{2} \rho_n v_n^2 \right) \right] = \mathbf{J} \cdot \mathbf{E} + \sum_j H_j \quad (3)$$

where $e_n = p_n/(\gamma - 1) + \rho_n v_n^2/2$ is the internal energy per unit mass, s_{jn} the mass transfer rate between the charged fluid j and the neutral fluid, H_j the energy sinks or sources for the different fluids, \mathbf{B} the magnetic field, \mathbf{E} the electric field and \mathbf{J} the current given by $\mathbf{J} = \sum_j \alpha_j \rho_j \mathbf{v}_j$.

In the limit of small mass densities for the charged fluids, their inertia can be neglected. Also, the charged fluids are in thermal balance as their heat capacities are small. For the charged fluid j , the equations then reduce to

$$\frac{\partial \rho_j}{\partial t} + \frac{\partial}{\partial x}(\rho_j v_{x,j}) = -s_{jn}, \quad (4)$$

$$\alpha_j \rho_j \left(\mathbf{E} + \frac{\mathbf{v}_j \times \mathbf{B}}{c} \right) + \rho_j \rho_n K_{jn} (\mathbf{v}_n - \mathbf{v}_j) = 0, \quad (5)$$

$$H_j + G_{jn} = 0, \quad (6)$$

where α_j is the charge to mass ratio, K_{jn} the collision rate coefficient of the charged fluid j with the neutrals and G_{jn} the energy transfer rate per unit volume between the charged fluid and the neutral fluid. The expressions for K_{jn} and G_{jn} are given by Draine (1986). We use the reduced energy equation to calculate the temperatures of the ion and electron fluids. For the grain fluids, a hydrodynamic approximation with zero pressure is appropriate as the thermal velocity dispersion of the dust grains is small compared to the drift velocity with the neutrals.

The collisions of the charged particles with the neutral particles affect the evolution of the magnetic field. Using the reduced momentum equations for the charged fluids (Eq. 5) and the expression for the current \mathbf{J} , the electric field can be expressed as (Cowling 1956)

$$\mathbf{E} = -\mathbf{v}_n \times \mathbf{B} + r_{//} \frac{(\mathbf{J} \cdot \mathbf{B}) \mathbf{B}}{B^2} + r_H \frac{\mathbf{J} \times \mathbf{B}}{B} - r_{AD} \frac{(\mathbf{J} \times \mathbf{B}) \times \mathbf{B}}{B^2},$$

where $r_{//}$ is the resistivity along the magnetic field, r_H the Hall resistivity and r_{AD} the ambipolar resistivity. The expressions of the resistivities are given by e.g. Falle (2003) and depend strongly on the Hall parameter, $\beta_i = \alpha_i |\mathbf{B}| / K_{ni} \rho_n$, which is the ratio between the gyrofrequency of the charged fluid and collision frequency of the charged fluid with the neutrals. Substitution of the above expression into the Maxwell-Faraday equation then gives the magnetic induction equation

$$\frac{\partial \mathbf{B}}{\partial t} + \frac{\partial \mathbf{M}}{\partial x} = \frac{\partial}{\partial x} \mathbf{R} \frac{\partial \mathbf{B}}{\partial x}, \quad (7)$$

where $\mathbf{M} = \mathbf{v}_n \times \mathbf{B}$ is the hyperbolic magnetic flux and \mathbf{R} is the resistance matrix which depends on the Hall resistivity, the ambipolar resistivity, and the resistivity along the magnetic field. (For an expression for \mathbf{R} , see Falle (2003).)

Equations 1 - 7 are solved using the numerical scheme described by Falle (2003). This scheme uses a second-order hydrodynamic Godunov solver for the neutral fluid equations (Eqs. 1-3). The charged fluid densities are calculated using an explicit upwind approximation to the mass conservation equation (Eq. 4), while the velocities and temperatures are calculated from the reduced momentum and energy equations (Eq. 5 and 6). The magnetic field is advanced explicitly, even though this implies a restriction on the stable time step at high numerical resolution (Falle 2003).

2.2 Physical processes

The numerical code described in the previous section is quite general. In order to investigate the effects of dust grains in fast-mode shocks it is necessary to specify the source terms, i.e. the mass, momentum and energy transfer coefficients and the energy sources and sinks, to describe the relevant physics. The chemical network that we adopted is the one used by Pilipp, Hartquist, & Havnes (1990) and Pilipp & Hartquist (1994).

Mass transfer between the ion and electron fluids and the neutral fluid is due to cosmic ray ionisation at a rate of 10^{-17} s^{-1} , electron recombination with Mg^+ , dissociative recombination with HCO^+ and recombination of ions on charged grains. Here we have assumed that the main gas phase ions are Mg^+ and HCO^+ (Oppenheimer & Dalgarno 1974). The cross-section for these recombination reactions are taken from Pilipp, Hartquist, & Havnes (1990).

Mass is also transferred between the ion and electron fluids and the grain fluids due to ion neutralisation on grain surfaces. Ions and electrons stick to dust grains upon colliding with them. Also, they pass on their charge with unit efficiency. The grain charge then critically depends on the electron-grain and ion-grain collision rates (which themselves depends on the electron density and temperature, the ion density and temperature, and the ion-grain relative streaming speed). The average grain charge is evaluated following Havnes, Hartquist, & Pilipp (1987). Individual grains can have a charge that differs from the average value, but it is mostly within one unit of the average (Elmegreen 1979).

Different radiative cooling processes for the neutral and electron fluids are included in the code. The elec-

tron gas is cooled by the excitation and subsequent de-excitation of molecular hydrogen (e.g. DRD). This process only becomes important when the electron fluid temperature exceeds ≈ 1000 K. In the neutral gas, the dominant cooling processes are associated with O, CO, H₂ and H₂O. The radiative transitions for atomic oxygen, i.e. OI lines, are calculated using the procedure of DRD. The radiative losses from excited rotational-vibrational states of molecular hydrogen are a fit to the data presented by Hartquist, Dalgarno, & Oppenheimer (1980), while those of CO are calculated by using Hollenbach & McKee (1979). Finally, we use Neufeld & Melnick (1987) to calculate the losses due to rotational transitions in H₂O. The heating rate of the neutral gas by cosmic rays is from DRD. We have not included any radiative losses for the ion fluid. From Eq. 6 and using the expression for G_i (Draine 1986) we find that the ion temperature, T_i , is given by

$$T_i = T_n + \frac{m_n}{3k_B}(\mathbf{v}_n - \mathbf{v}_i)^2, \quad (8)$$

where T_n is the neutral temperature, m_n the neutral particle mass and k_B the Boltzmann constant.

2.3 Initial conditions

The initial conditions of our simulations are adopted from DRD and similar studies such as Wardle (1998) and Chapman & Wardle (2006). This allows a comparison of our results with those of these studies.

The neutral fluid has a number density of $n_H = 10^4$ cm⁻³ or $n_H = 10^6$ cm⁻³ and is composed mainly of molecular hydrogen so that $m_n \approx 2m_H$. Small amounts of other neutral species such as O, CO, and H₂O are also present. The initial abundances of O, CO, and H₂O are taken to be $4.25 \times 10^{-4} n_H$, $5 \times 10^{-5} n_H$ and 0 respectively. However, as the abundances of O and H₂O evolve substantially as gas is heated, the abundances of the important coolants are recalculated at every time-step. The dominant ions within the gas are assumed, as mentioned above, to be HCO⁺ and Mg⁺. The ion mass is then $m_i \approx 30m_H$. Also, we assume that the ions are only singly ionised.

The dust grains are all assumed to be spherical with a radius of $a_g = 0.4 \mu\text{m}$ and a mass of 8.04×10^{-13} g (where the density of the grains is taken 3 g cm⁻³). The grain to hydrogen mass ratio in the unshocked region has the canonical value of 0.01. The densities of the ion and electron fluids and the average grain charge are calculated from ionisation equilibrium. For the temperatures that we adopt, i.e. $T_n = 8.4$ K for $n_H = 10^4$ cm⁻³ and $T_n = 26.7$ K for $n_H = 10^6$ cm⁻³, the average grain charge is quite close to $-e$ and the electron and ion number densities are roughly the same, i.e. $n_e \approx n_i$.

In the interstellar medium the magnitude of the magnetic field scales roughly as $B \approx 1 \mu\text{G}(n_H/\text{cm}^{-3})^{-1/2}$ (see DRD) so that $B = 10^{-4}$ G for $n_H = 10^4$ cm⁻³ and $B = 10^{-3}$ G for $n_H = 10^6$ cm⁻³. The Alfvén speed of the gas is then the same at both densities, i.e. $v_A = 2.2$ km s⁻¹. In the far upstream region the magnetic field lies in the x, y -plane and makes an angle of 30°, 45°, 60° or 90° (perpendicular shock) with the x -axis. We assume that a shock is propagating in the positive x -direction with a speed of 25 km s⁻¹. Such a shock is a strong fast-mode shock with an Alfvénic Mach number of $M_A \approx 11.5$.

Using the upstream fluid properties, the properties far downstream of the shock are calculated from the Rankine-Hugoniot relations for an isothermal, magnetised shock. For our initial shock structure we assume that the shock is a discontinuity at $x = 0$ separating the upstream and downstream properties. We follow the evolution of the shock to steady state within the shock frame.

2.4 Computational details

The size of the computational box is assumed to be a few times the shock width. By balancing the ion-neutral drag force with the Lorentz force, we can estimate the shock thickness (e.g. Draine & McKee 1993)

$$L_i = 7 \times 10^{15} \left(\frac{v_A}{\text{km s}^{-1}} \right) \left(\frac{10^{-2} \text{cm}^{-3}}{n_i} \right) \text{cm}, \quad (9)$$

where v_s is the shock speed. However, the grain-neutral friction is comparable to the ion-neutral friction for

$$\frac{\rho_i}{\rho_g} < \frac{K_{gn}}{K_{in}},$$

or

$$\chi < 3 \times 10^{-9} \left(\frac{v_s}{\text{km s}^{-1}} \right),$$

where we substituted the expressions for the collision rates with the neutrals (Draine 1986) and assumed the relative speed between the neutrals and the grains to be of the order $v_s/2$. This constraint is fulfilled in the heated precursor for both densities and the shock thickness is determined by the grain-neutral drag. The expression for the shock width is similar to Eq. 9 and is given by

$$L_g = 3 \times 10^8 \chi \left(\frac{v_s}{\text{km s}^{-1}} \right)^{-1} L_i. \quad (10)$$

Values of χ appropriate for the precursor must be used. Flower, Pineau des Forêts, & Hartquist (1985) first pointed out that chemistry leads to a large drop in χ in the precursor of many shocks. The numerical domain is then chosen to be $-10L_g \leq x \leq 10L_g$ with a free-flow boundary condition at the downstream side and fixed inflow at the upstream boundary. We use a uniform grid with 400 cells.

As our initial conditions are discontinuous, the inertia of the charged fluid, even the ions, cannot be neglected during the initial stages of the evolution. However, the inertial phase of the charged fluid is short compared to the time to approach a steady configuration (e.g. Roberge & Ciolek 2007). Although the inertial phase does not affect the final steady shock structure here, this effect should not be ignored for some other time-dependent models.

3 C-TYPE SHOCK MODELS

In this section we present steady C-type shock structures for large single-sized grains. First we discuss perpendicular shocks and then shocks propagating at an oblique angle with the magnetic field.

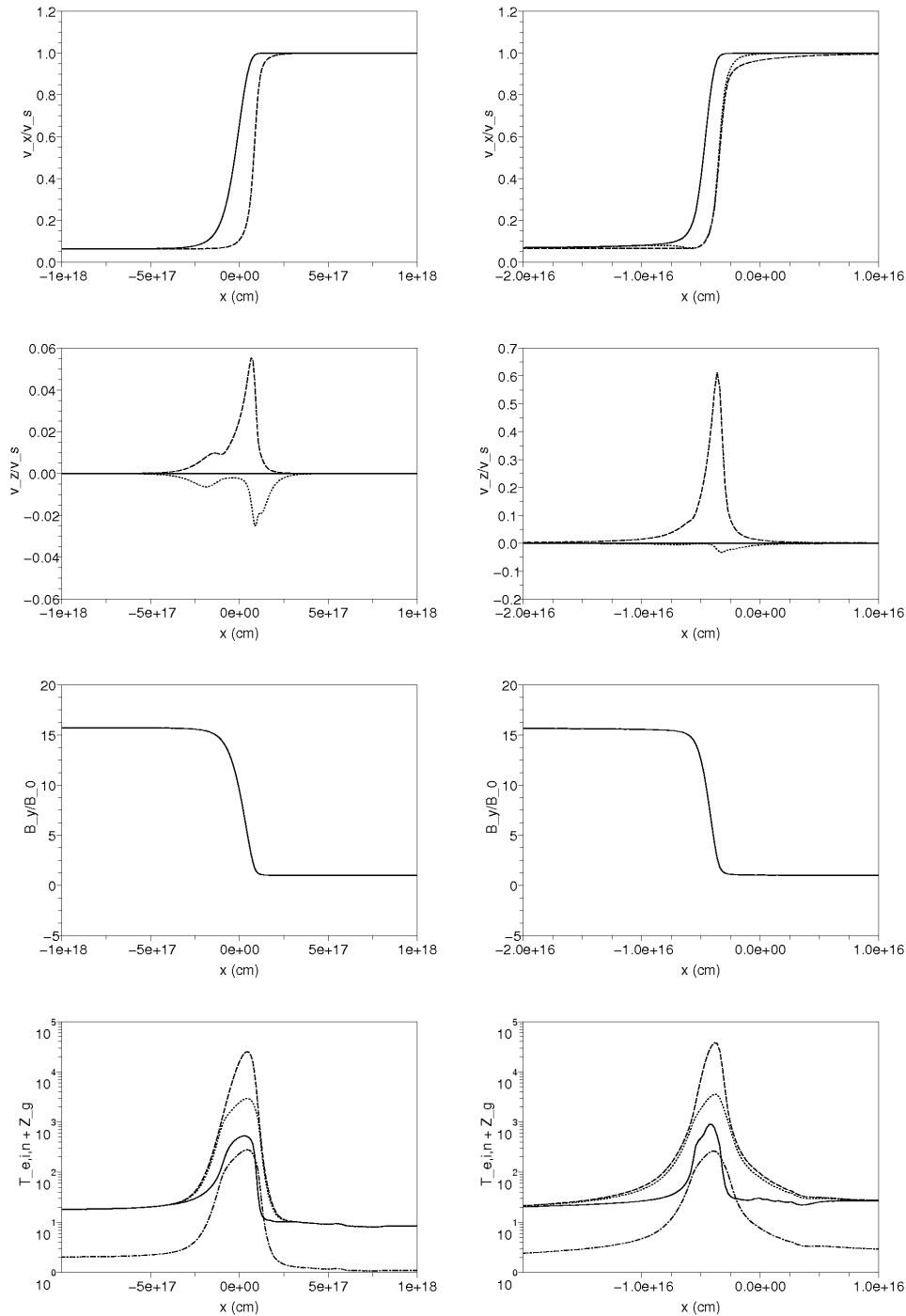


Figure 1. The shock structure for a perpendicular shock propagating in a quiescent region with $n_{\text{H}} = 10^4 \text{ cm}^{-3}$ (left) and $n_{\text{H}} = 10^6 \text{ cm}^{-3}$ (right). From top to bottom we plot the velocity in the x -direction and z -direction for the neutrals (solid), ions/electrons (dashed) and grains (dotted), the tangential magnetic field and the temperatures of the ions (dashed), electrons (dotted) and the neutrals (solid) as well as the absolute value of the grain charge (dash-dotted). The velocities are normalised with respect to the shock speed and the magnetic field to the total upstream magnetic field.

3.1 Perpendicular shocks

Figure 1 shows the structures in multiple flow variables for perpendicular shocks at different densities. It is clear that both shock structures represent C-type shocks. As our models are similar to DRD, we can compare our results with figs. 2 and 3 of DRD. Although the shapes of the shocks are

qualitatively similar, our shock widths are about 4 times larger than in DRD. This is due to a lower fractional ionisation in our models which is a consequence of including the chemistry governing the ionisation rather than assuming a constant ion flux as DRD did. The drag force of the charged particles on the neutrals is then lower as well and is balanced by the magnetic pressure over a larger length scale. A

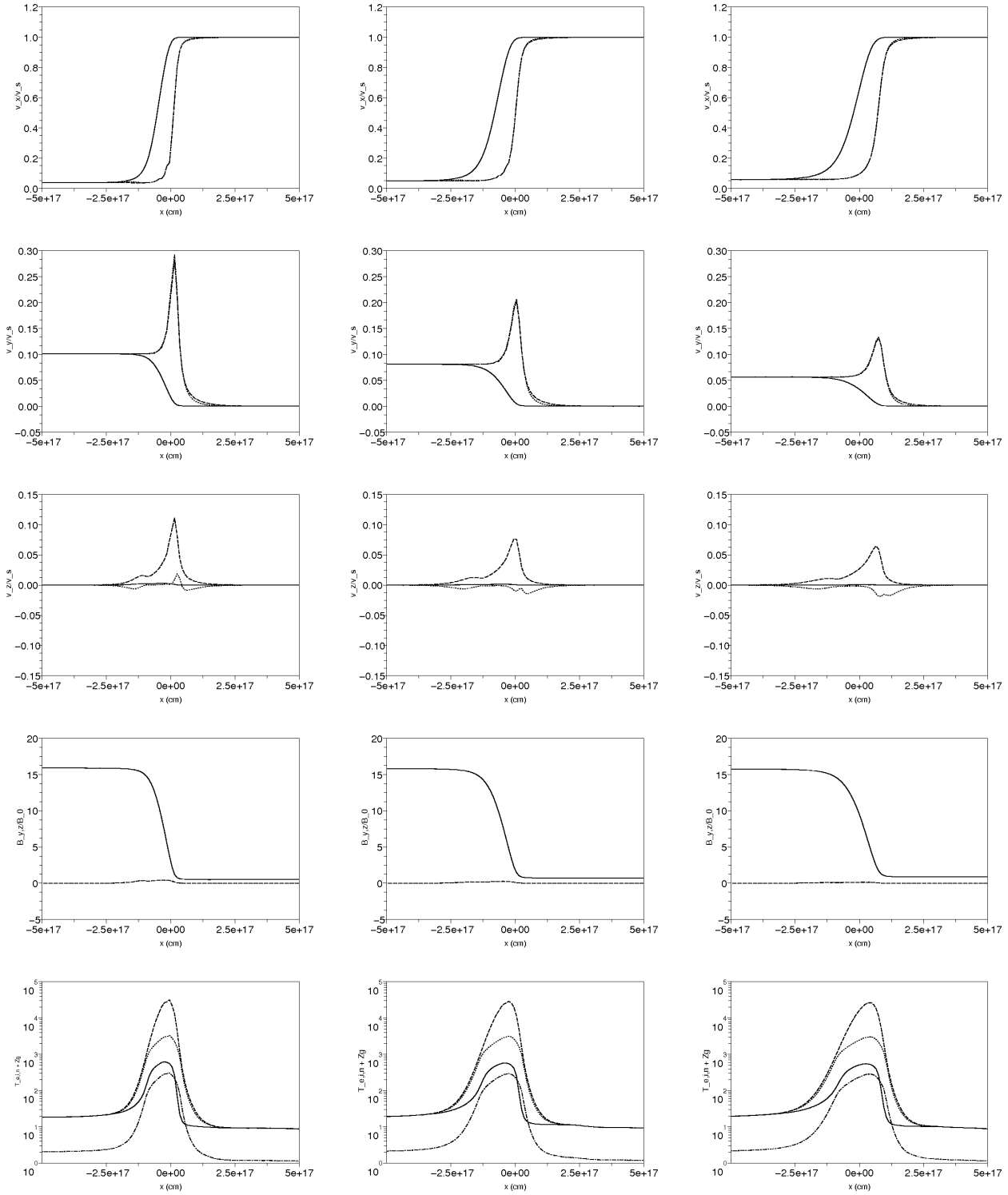


Figure 2. The shock structure for an oblique shock propagating at an angle of 30° (left), 45° (middle) and 60° (right) with the magnetic field in a quiescent region with $n_H = 10^4 \text{cm}^{-3}$. From top to bottom we plot the velocity in the x -direction, y -direction and z -direction for the neutrals (solid), ions/electrons (dashed) and grains (dotted), the tangential magnetic field in the y -direction (solid) and z -direction (dashed), and the temperatures of the ions (dashed), electrons (dotted) and the neutrals (solid) as well as the absolute value of the grain charge (dash-dotted). The velocities are normalised with respect to the shock speed and the magnetic field to the total upstream magnetic field.

consequence of the larger shock widths is that the gas has more time to radiate away its energy. The maximum temperature of the neutrals within the shock front is only 530 K for $n_{\text{H}} = 10^4 \text{cm}^{-3}$ and 905 K for $n_{\text{H}} = 10^6 \text{cm}^{-3}$, while DRD found 1223 K and 1334 K respectively.

Figure 1 shows that the speed of the grains relative to the neutrals is less than the speed of the ions relative to the neutrals. The difference in relative speeds is due to the different response of the charged fluids to the Pedersen along $\mathbf{E}' (= \mathbf{E} + \mathbf{v}_{\text{n}} \times \mathbf{B})$ and Hall current along $\mathbf{E}' \times \mathbf{B}$ within the shock front. From Eq. 5 we find

$$\frac{\mathbf{v}_{\text{j}} - \mathbf{v}_{\text{n}}}{c} \approx \frac{\beta_j^2}{1 + \beta_j^2} \left(\frac{\mathbf{E}' \times \mathbf{B}}{B^2} \right) + \frac{\beta_j}{1 + \beta_j^2} \left(\frac{\mathbf{E}'}{B} \right), \quad (11)$$

where β_j is the Hall parameter of the charged fluid. For electrons and ions with $|\beta_{e,i}| \gg 1$, the particles are tied to the magnetic field and

$$\frac{\mathbf{v}_{e,i} - \mathbf{v}_{\text{n}}}{c} \approx \frac{\mathbf{E}' \times \mathbf{B}}{B^2}.$$

At the other extreme, $|\beta_j| \ll 1$, the charged particles move with the neutrals. For the $n_{\text{H}} = 10^6 \text{cm}^{-3}$ models, the grains have a Hall parameter ranging from -0.1 (the upstream value) to a minimum of -1.5 within the shock front. For these values, the \mathbf{E}' term has a non-negligible contribution to the drift velocity. For the x -component of the velocity of the grains, this term only becomes important when the grains switch from moving with the neutrals to moving with the ions and electrons (see Fig. 1). The z -component of the \mathbf{E}' term, however, has a larger contribution to the drift forcing the grains to move with the neutrals. The lower density model exhibits this effect to a lesser extent as the grain Hall parameter lies between -1 and -20. Then the \mathbf{E}' term is less important and provides only a small contribution to the drift.

The velocity difference between the ions and electrons with the neutrals determines the temperature of the charged particles through collisional heating. The maximum velocity difference in the models is $\approx v_s$ giving a maximum ion temperature of a few times 10^4 K. Electron cooling becomes important at temperatures of about 1000 K reflected in a considerably lower electron temperature at roughly 3×10^3 K. The electron temperature within the shock front is important for the dynamics of the shock as the average grain charge is

$$Z_g e \approx -\frac{4k_b T_e a_g}{e}, \quad (12)$$

for $|Z_g| \gg 1$ and $n_g |Z_g| \ll n_e$ (e.g. Draine 1980). Otherwise, the average grain charge is roughly -1. From Fig. 1 we find that the average grain charge follows this dependence on the electron temperature with the average grain charge reaching maximum values of about -250.

3.2 Oblique shocks

For a finite magnetic field component parallel to the shock propagation and a non-zero Hall conductivity, the Hall current along $\mathbf{E}' \times \mathbf{B}$ has a component parallel to the propagation direction of the shock. As the total current in that direction is zero if the shock is steady, the Hall current needs

to be balanced by the Pedersen current (along \mathbf{E}'). This Pedersen current gives rise to the rotation of the magnetic field around the shock propagation (Pilipp & Hartquist 1994). Significant rotation occurs when the Hall conductivity is larger than the Pedersen conductivity (Wardle 1998).

For the $n_{\text{H}} = 10^4 \text{cm}^{-3}$ models, the Hall conductivity is always smaller than the Pedersen conductivity and there is no significant rotation of the magnetic field (see z -component of magnetic field in Fig. 2). The rotation increases marginally as the angle, θ , between the direction of shock propagation and the magnetic field decreases. The other shock properties, also, do not change significantly with θ . The temperatures of the different fluids and the average grain charge are similar to the ones found for the perpendicular shock. These results agree well with the θ -dependence of the steady shock structure found by Chapman & Wardle (2006). The similarity of the shock structure for different values of θ results from the minor contribution of the grains to the drag force on the neutrals. The grains do not determine the dynamics and drift with the other charged species.

Significant differences, however, are seen in the $n_{\text{H}} = 10^6 \text{cm}^{-3}$ models. Here, the grains are the dominant contributors to the drag force on the neutrals. Furthermore, there is a significant charge separation giving rise to a large Hall conductivity. In Fig. 3 we see that there is a substantial rotation of the magnetic field. Also the magnetic field upstream is no longer a stable node, but a spiral node as the Hall conductivity changes wave propagation upstream (Wardle 1998; Falle 2003). As for $n_{\text{H}} = 10^4 \text{cm}^{-3}$, the rotation decreases for larger θ , while the shock width increases.

The rotation of the magnetic field has large consequences for the drift velocity of the charged particles. Figure 3 shows that the velocity structure changes considerably with θ . Also, the grains move significantly differently than the ions and electrons, especially in the $\theta = 30^\circ$ model (see Fig. 3). Along the propagation direction, electrons and ions are decelerated immediately. The grains, however, are initially accelerated before being decelerated. Furthermore, they lag the ions and electrons. To drift in the direction opposite to the ions and electrons, the grains motion must be dominated by the \mathbf{E}' term in Eq. 11 and E'_x must be in the same direction as the x -component of $\mathbf{E}' \times \mathbf{B}$. The large differences in drift velocity are expected as the rotation of the magnetic field is induced by a charge separation (and thus large Hall conductivity). For larger θ , the Hall conductivity and rotation decrease, so that the ions, electrons, and grains move more together. As expected, the velocity profile converges to the perpendicular shock structure (see Fig. 1 and 3).

4 MULTIPLE GRAIN SPECIES

In Sect. 3 we have assumed a single-sized grain fluid. In molecular clouds, however, the dust has a grain-size distribution given by (Mathis, Rumpl, & Nordsieck 1977)

$$\frac{dn}{da} \propto a^{-3.5}, \quad (13)$$

where dn is the number density of grains with radii between a and $a + da$. To take into account the effect of multiple dust species, we include an additional small-grain fluid with

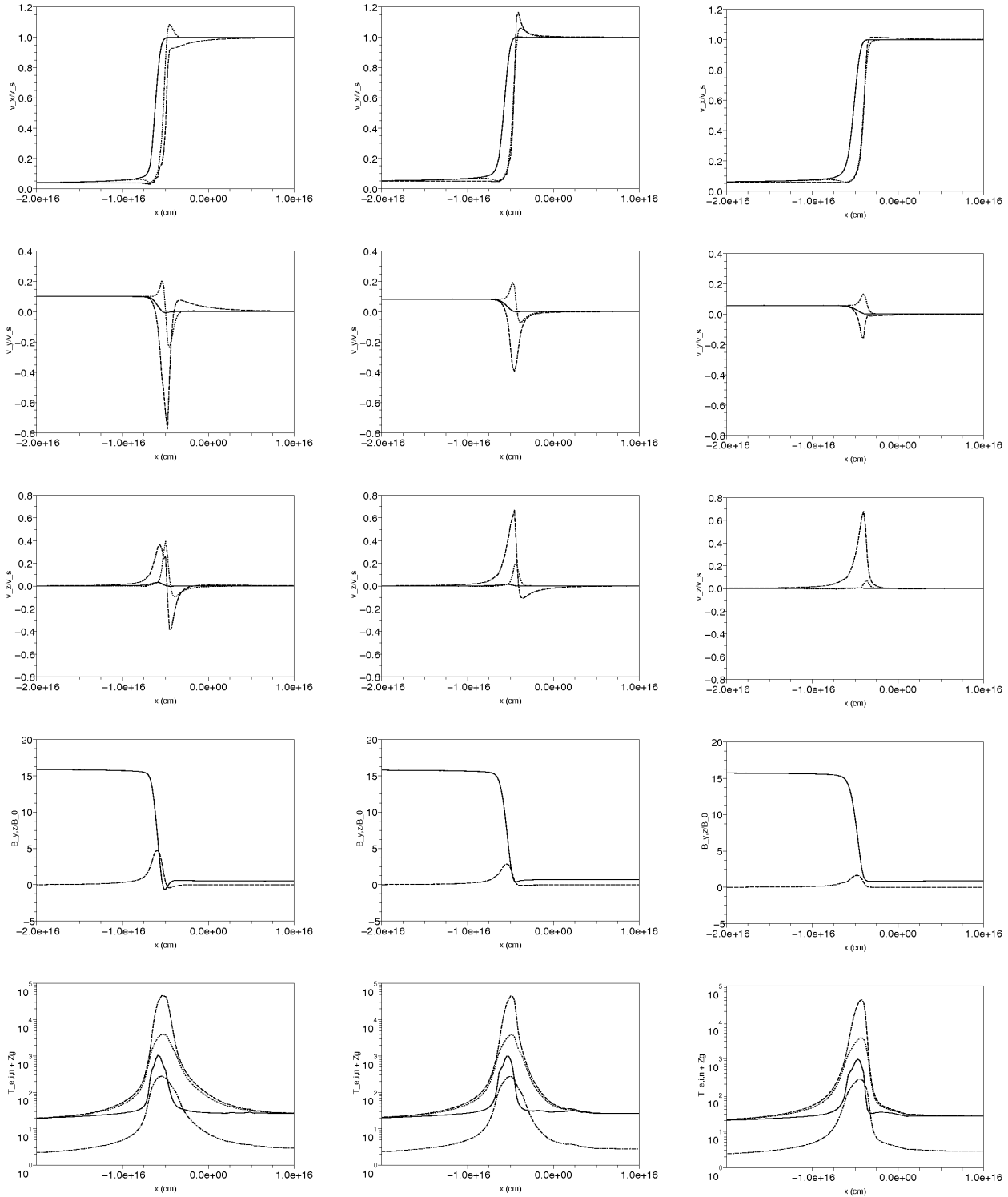


Figure 3. Same as in Fig. 2, but with an upstream density of $n_H = 10^6 \text{ cm}^{-3}$.

$a_s = 0.04 \mu\text{m}$ (i.e. $a_s = a_g/10$) and $m_s = 8.03 \times 10^{-16} \text{ g}$ (or $m_s = m_g/1000$). The total mass density of the grain fluid, $\rho_s + \rho_g$, is assumed to be 1% of the neutral mass density (as in our previous models). With the adopted grain-size distribution most of the mass is in the small grain fluid. Furthermore, the small grains dominate the grain-neutral friction

and, thus, the shock dynamics as the collision coefficient between grains and neutrals is proportional to $a_{g,s}^2/m_{g,s}$ (see Draine 1986). From Fig. 4, we see that the shock width is indeed, as expected from Eq. 10, an order of magnitude smaller than for the model with single-sized large grains.

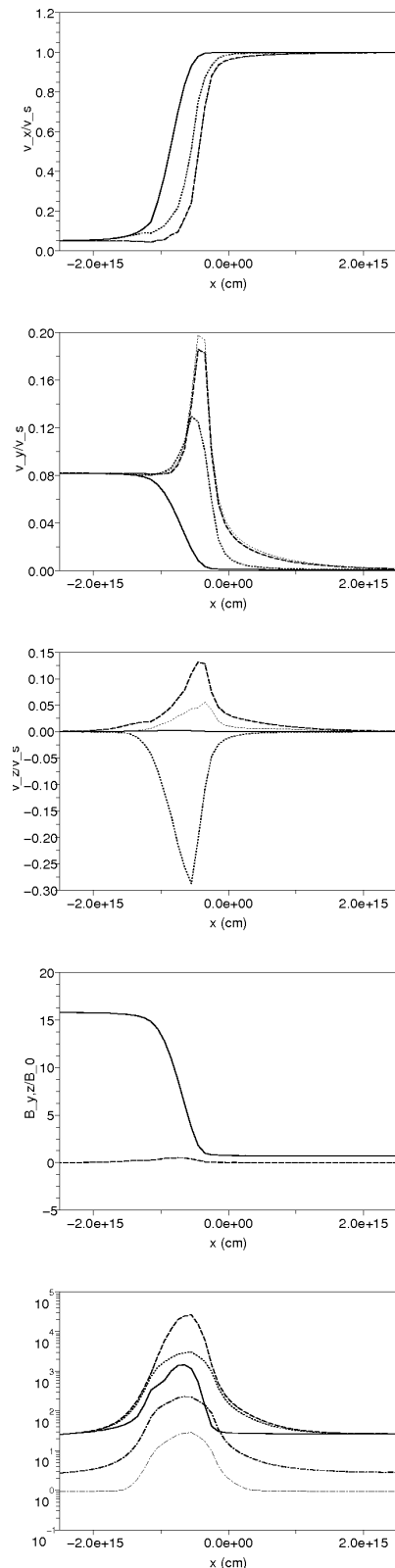


Figure 4. Similar to the 45° model of Fig. 3, but for two grain fluids. The small grains are indicated on the velocity components figures with a thin-dotted line, while their average charge is given by a thin dashed-dotted line.

Although the small grains have an average charge about an order of magnitude smaller than the large grains (see Eq. 12), the small grains have a larger Hall parameter and are strongly coupled to the magnetic field. The velocity plots in Fig. 4 show that the small grains move with the electrons and ions, while the large grains move with velocities between those of the neutrals and the other charged particles. The grain charge density is dominated by the small grains and free electrons are depleted from the gas phase (i.e. $n_i \gg n_e$). The charge separation between the charged particles is thus small and the Hall conductivity is too. The rotation of the magnetic field out of the plane is then negligible. Also, the upstream magnetic field is no longer a spiral node, but a stable node.

The inclusion of a second grain species thus changes the shock structure considerably. Including additional grain species will further affect the shock structure as more dust grains are loading the magnetic field lines. Then the signal speed at which disturbances propagate through the charged fluid decreases. For small PAH abundances the signal speed is close to 25 km s^{-1} (Flower & Pineau des Forêts 2003) leading to the possibility that the resulting shock is a J-type shock in which the grain inertia cannot be neglected.

5 SUMMARY AND DISCUSSIONS

In this paper we have presented 1D time-dependent multi-fluid MHD simulations of perpendicular and oblique C-type shocks in dusty plasmas. We have included in our numerical code relevant mass transfer processes, such as electron recombination with Mg^+ and dissociative recombination with HCO^+ , and radiative cooling by O, CO, H_2 and H_2O . Also, the mass and charge transfer from ions and electrons to the dust grains is taken into account to calculate the average grain charge. Our models are the first of oblique fast-mode shocks in dense molecular clouds in which a fluid treatment of grain dynamics has been combined with a self-consistent calculation of the thermal and ionisation balances including appropriate microphysics. We have performed simulations with single-sized and with two dust grains species in plasmas of different density.

Dust grains do not change the shock dynamics much at $n_H = 10^4 \text{ cm}^{-3}$ and the shock structures for oblique and perpendicular shocks are quite similar. Grains, however, dominate the shock dynamics at high densities ($n_H = 10^6 \text{ cm}^{-3}$). For oblique shocks, the magnetic field in the shock front is not confined to the upstream magnetic field plane. The amount of rotation obtained depends on the Hall and Pedersen conductivities. For single-sized grains the rotation is significant and increases with smaller θ as the Hall conductivity in these models is comparable to the Pedersen conductivity. For some models, the magnetic field at the upstream side of the shock even spirals around the direction of shock propagation. When we include an additional small grain species, the rotation mostly disappears. The small grains which carry most of the charge move with the ions and electrons reducing the Hall conductivity. Our models corroborate the main qualitative conclusions of previous studies (DRD Pilipp & Hartquist 1994; Wardle 1998; Chapman & Wardle 2006; Guillet, Pineau des Forêts, & Jones 2007), showing that our numerical method is efficient, rigorous, and robust.

In addition, we have succeeded in taking a significant step by developing the first oblique shock code capable of producing reliable results for comparisons with observations. Previous oblique shock models were restricted by less rigorous treatments of either the grain dynamics or the thermal and ionisation balances.

However, our model does have some restrictions. Firstly, we determine the drift velocities of the grains solely by balancing the grain-neutral friction with the Lorentz force and neglect their inertia. While small dust grains can be considered inertialess, large grains have a drag length, i.e. the length scale for gas drag to decelerate the grains, that in some cases is comparable to the length scale for magnetic field compression (Ciolek & Roberge 2002). Therefore, large grain inertia cannot always be neglected. Secondly, for small grains, the average grain charge is close to the elementary charge. As there is some fluctuation around the average, a fraction of the small grains has a zero or even positive charge. The neutral grains decouple from the magnetic field, while the positive grains drift in a different direction to the negative grains. Although this fluctuation around the average grain charge changes the shock structure, its effect is only minimal (Guillet, Pineau des Forêts, & Jones 2007).

A time-dependent method is not only robust (even for non-equilibrium conditions) for finding steady state shock structures. It is also vital for modelling transient phenomena. In the vicinity of protostellar objects the abundance of SiO is significantly enhanced (e.g. Martín-Pintado, Bachiller, & Fuente 1992; Jiménez-Serra et al. 2004). It is thought that the SiO emission arises from the interaction of a protostellar jet with local dense clumps (Lefloch et al. 1998). Grain sputtering within C-type shocks releases the SiO depleted on the grains back into the gas phase (Caselli, Hartquist, & Havnes 1997; Schilke et al. 1997). Numerical models using steady C-type shocks indeed show good agreement with recent observations of SiO line intensities in the L1157 and L1448 molecular outflows (Gusdorf et al. 2008a,b). However, it is doubtful that shocks interaction with dense clumps have reached steady state. In subsequent papers, we will study the interaction of C-type shocks with dense clumps and include grain sputtering to calculate the SiO emission.

ACKNOWLEDGEMENTS

We thank the anonymous referee for a report that helped to improve the manuscript. SVL gratefully acknowledges STFC for the financial support.

REFERENCES

- Bally J., Lada C. J., 1983, *ApJ*, 265, 824
 Caselli P., Hartquist T. W., Havnes O., 1997, *A&A*, 322, 296
 Chapman J. F., Wardle M., 2006, *MNRAS*, 371, 513
 Ciolek G. E., Roberge W. G., 2002, *ApJ*, 567, 947
 Cowling T. G., 1956, *MNRAS*, 116, 114
 Draine B. T., 1980, *ApJ*, 241, 1021
 Draine B. T., 1986, *MNRAS*, 220, 133
 Draine B. T., McKee C. F., 1993, *ARA&A*, 31, 373
 Draine B. T., Roberge W. G., Dalgarno A., 1983, *ApJ*, 264, 485
 Elmegreen B. G., 1979, *ApJ*, 232, 729
 Falle S. A. E. G., 2003, *MNRAS*, 344, 1210
 Flower D. R., Pineau des Forêts G., 2003, *MNRAS*, 343, 390
 Flower D. R., Pineau des Forêts G., Hartquist T. W., 1985, *MNRAS*, 216, 775
 Guillet V., Pineau des Forêts G., Jones A. P., 2007, *A&A*, 476, 263
 Gusdorf A., Cabrit S., Flower D. R., Pineau des Forêts G., 2008a, *A&A*, 482, 809
 Gusdorf A., Pineau des Forêts G., Cabrit S., Flower D. R., 2008b, *A&A*, 490, 695
 Hartquist T. W., Dalgarno A., Oppenheimer M., 1980, *ApJ*, 236, 182
 Havnes O., Hartquist T. W., Pilipp W., 1987, *ppic.proc*, 389
 Hollenbach D., McKee C. F., 1979, *ApJS*, 41, 555
 Jiménez-Serra I., Martín-Pintado J., Rodríguez-Franco A., Marcelino N., 2004, *ApJ*, 603, L49
 Lefloch B., Castets A., Cernicharo J., Loinard L., 1998, *ApJ*, 504, L109
 Martín-Pintado J., Bachiller R., Fuente A., 1992, *A&A*, 254, 315
 Mathis J. S., Rumpl W., Nordsieck K. H., 1977, *ApJ*, 217, 425
 Mestel L., Spitzer L., Jr., 1956, *MNRAS*, 116, 503
 Mullan D. J., 1971, *MNRAS*, 153, 145
 Neufeld D. A., Melnick G. J., 1987, *ApJ*, 322, 266
 Oppenheimer M., Dalgarno A., 1974, *ApJ*, 192, 29
 Pilipp W., Hartquist T. W., Havnes O., 1990, *MNRAS*, 243, 685
 Pilipp W., Hartquist T. W., 1994, *MNRAS*, 267, 801
 Roberge W. G., Ciolek G. E., 2007, *MNRAS*, 382, 717
 Schilke P., Walmsley C. M., Pineau des Forêts G., Flower D. R., 1997, *A&A*, 321, 293
 Wardle M., 1998, *MNRAS*, 298, 507